Hybrid Approaches to PAPR, BER, and PSD Optimization in 6G OTFS: Implications for Healthcare

Arun Kumar, Sumit Chakravarthy, Nishant Gaur, and Aziz Nanthaamornphong

***Abstract*—The envisioned smart hospital framework leveraging the sixth-generation (6G) technology aims to enhance healthcare services by ensuring reliable communication across various wireless channel conditions, including both line-of-sight and obstructed paths. However, the traditional orthogonal frequency division multiplexing (OFDM) approach, used in 4G and 5G, struggles with the high Doppler shifts associated with dynamic environments, presenting challenges for burgeoning smart hospital demands. To address this, orthogonal time frequency space (OTFS) modulation is proposed. The OTFS operates effectively across both stationary and highly mobile channels by manipulating delay and Doppler domains. Nevertheless, a high peak-to-average power ratio (PAPR) remains a critical challenge for OTFS implementation within 6G smart hospitals. Elevated PAPR levels can reduce power amplifier efficiency, causing them to operate outside their ideal linear range and impairing battery performance. They also contribute to signal distortion, increased interference, and suboptimal spectrum utilization, which can undermine wireless communication and data integrity. To mitigate the PAPR issue in OTFS, this work introduces a hybrid algorithm that integrates the benefits of the Riemann matrix optimal phase element-based partial transmission sequence (PTS) and selective mapping (SLM), along with A and μ-law complementary algorithms. This study compares the performance of the proposed hybrid algorithm with traditional PAPR reduction techniques by evaluating metrics such as PAPR, bit error rate (BER), and power spectrum density (PSD) within the Rician and Rayleigh fading channels. Simulation outcomes indicate that the hybrid algorithm achieves superior PAPR, BER, and PSD performance with only a marginal increase in complexity when compared with the established methods.**

***Index Terms*—6G based smart hospital, hybrid algorithms, OTFS, PAPR, PSD.**

I. Introduction

THE sixth generation of wireless communication technology, commonly referred to as 6G, heralds a new era characterized by heightened data transmission speeds, diminished latency, and more sophisticated levels of connectivity. In the healthcare realm, smart hospitals harness the capabilities of 6G to revolutionize medical services through the integration of groundbreaking technologies such as artificial intelligence (AI), the Internet of things (IoT), and instantaneous data monitoring. This integration is poised to significantly refine the quality of patient treatment, streamline resource management, and augment the overall efficiency of hospital operations [1]. With the increase in the aging population worldwide, high quality of health care services is one of the most important constraints. Conventional hospitals require large infrastructure and workforce to accommodate an increasing number of patients. In the COVID-19 pandemic situation, it has been seen that the present conventional hospital cannot provide better health services owing to a lack of infrastructure and trained medical health care. It was also observed that many diseases can be perfectly cured while sitting at the hospital if proper guidance and monitoring are provided. Hence, it is important to use advanced technologies in conventional hospitals to make them smart [2]. In the present scenario, the use of advanced techniques, such as 4G radio and medical wearable devices, has raised the standard of health services. For example, one can obtain information about the specialist doctor for a particular disease and take the consultation by sitting at home. This will increase the trust and understanding between doctors and patients. However, the hospital is still not properly utilizing advanced sixth-generation (6G) integration. Otherwise, it would be useful for remote health services [3]. 6G revolutionizes smart hospitals by enabling unprecedented data speed, ultralow latency, and seamless connectivity. This empowers the real-time monitoring of patients, high-definition telemedicine, and advanced robotic surgeries. With enhanced network reliability, 6G ensures swift communication between medical devices, AI-assisted diagnostics, and smart infrastructure, fostering a new era of healthcare innovation for improved patient care, research, and operational efficiency [4]. The 6G-based smart hospital can solve several problems in health care and enhance the quality of service, including health monitoring, home consultation, remote surgical operation, and consultation with the best doctors around the world. Smart hospitals will revolutionize healthcare services by digitizing the infrastructure and combining all electronics and physical assets in a unified framework. Hence, smart hospitals can provide real-time analysis of patient conditions and prevent many uncertainties [5]. The efficacy of smart hospitals employing

Manuscript received December 16, 2023; approved for publication March 2, 2024; approved for publication by WU, YIK CHUNG Division 2 Editor, May 21, 2024.

A. Kumar is with Department of Electronics and Communication Engineering, New Horizon College of Engineering, Bengaluru, India, email: dr.arunk.nhce@newhorizonindia.edu.

S. Chakravarthy is with Department of Electrical Engineering and Computer Engineering, Kennesaw State University, GA, USA, email: schakra2@kennesaw.edu.

N. Gaur is with Department of Physics, JECRC University, India, email: nishant.gaur@jecrcu.edu.in.

A. Nanthaamornphong is with College of Computing, Prince of Songkla University, Thailand, email: aziz.n@phuket.psu.ac.th.

A. Nanthaamornphong is the corresponding author.

Digital Object Identifier: 10.23919/JCN.2024.000027

1229-2370/24/$10.00 © 2024 KICS

6G technology hinges on meeting a set of critical criteria, which include extensive bandwidth, accelerated data transfer rates, steadfast connectivity, devices that utilize less power, and minimal latency. The implementation of a sophisticated multi-carrier waveform within the 6G infrastructure is pivotal for fulfilling these smart hospital requirements. Consequently, the development of a novel waveform in the physical layer is paramount [6]. Currently, the race for the 6G waveform is going all around the world. the latest waveform scheme used in 4G and 5G is orthogonal frequency division multiplexing (OFDM). However, OFDM has some drawbacks, such as bandwidth loss due to the use of cyclic prefixes (CP), inability to support gigantic devices, latency of approximately 20 to 30 ms, and high peak-to-average power ratio (PAPR) [7]. The orthogonal time frequency space (OTFS) modulation is emerging as a leading candidate for 6G waveforms owing to its multiple benefits. These include reduced latency, robust performance in high-speed environments, enhanced spectral efficiency, and ability to support rapid data transmission rates [8]. Despite its high receiver complexity, OTFS modulation is considered suitable for 6G due to its unique capabilities. OTFS offers robustness against delay spread and Doppler shift, making it resilient in high-mobility scenarios, a key consideration for 6G's focus on ultra-reliable and low-latency communication. Additionally, OTFS's high spectral efficiency and potential for massive connectivity align with 6G's goals of accommodating diverse applications, including IoT and AI-driven services. While OTFS requires sophisticated signal processing, advancements in hardware capabilities and signal processing algorithms are expected to mitigate complexity challenges, making it a promising candidate for next-generation wireless systems like 6G. The OTFS can also be designed using pre- and post-processing components in an advanced multi-carrier waveform. The OTFS signals are implemented in the Doppler domain, which transforms rapidly varying fading into a slow, flat-fading channel. This implies that the signal in the DD domain offers a higher time invariance than the signal in the frequency-time domain. It is also seen that the signal in DD exhibits numerous advantages, such as high robustness of the system, sparsity, solidity, and orthogonality, which play an important role in lowering the channel assessment overhead in the multipath fast-fading channel. Hence, OTFS can be integrated with a 6G radio-based smart hospital [9]. OTFS modulation offers distinct advantages over OFDM for healthcare applications. OTFS's resilience to delay spread and Doppler effects ensures reliable communication in dynamic environments, critical for wearable health monitoring devices in hospitals. Its ability to handle time-varying channels and mitigate multipath propagation enhances signal robustness, crucial for maintaining accurate and timely transmission of patient data. Moreover, OTFS's high spectral efficiency optimizes bandwidth usage, accommodating the increasing demand for wireless healthcare services without sacrificing performance. These advantages make OTFS well-suited for healthcare applications, supporting seamless integration of wireless technologies to enhance patient care and healthcare delivery efficiency. However, a high PAPR is seen as one of the biggest problems in the implementation of OTFS in 6G smart hospitals. High PAPR in OTFS implementation in 6G smart hospitals causes performance degradation of the power amplifier used on the transmitting side of an OTFS framework [10]. Smart healthcare devices transmit the patient's information in the form of tiny packets and function with severe transmit power limitations to enhance battery life, which is crucial in smart hospital services to lower the cost of the applications. Hence, under the transmit power constraint, it is necessary to limit the power used in packet retransmission of the packets [11]. To enhance power optimization in smart healthcare, it is important to lower the high PAPR of the OTFS framework. Although it is impossible to completely eliminate PAPR in OTFS systems, it can be significantly reduced through the application of specialized PAPR reduction algorithms. Notably, the methods typically employed for PAPR reduction in OFDM are not directly transferable to OTFS because of the fundamental differences in their waveform structures [12]. The research presents a novel composite algorithm that integrates the advantages of both selected mapping (SLM) with companding (SLM+ companding) and partial transmit sequence (PTS) with companding (PTS+ companding). This innovative approach aims to enhance performance by combining the superior elements of these two methods. This hybrid approach is designed to improve the PAPR and power spectrum density (PSD) performance without substantially increasing the complexity of the system infrastructure while maintaining bit error rate (BER) integrity. In the proposed article, the main focus is to enhance the power amplifier performance by reducing the PAPR, which have several other advantages for 6G based smart hospital. First of all, an a 6G smart hospital, there will be a vast network of interconnected devices and sensors, ranging from medical equipment to patient monitoring systems. These devices will communicate wirelessly to transmit critical data in real-time. OTFS modulation, with its ability to combat Doppler shifts and delay spread, can offer robust communication channels. However, one of the challenges with OTFS is its high PAPR, which can lead to inefficiencies in power amplification. the proposed hybrid algorithms mitigate this issue, ensuring that communication within the smart hospital network is efficient and reliable. Secondly, OTFS modulation is designed to operate efficiently in time-varying and frequency-selective channels, characteristics often encountered in indoor environments like hospitals. By reducing PAPR through hybrid algorithms, more efficient use of the spectrum can be achieved. This is crucial in 6G networks where the spectrum will likely be even more crowded, with numerous devices competing for bandwidth within the hospital environment. Thirdly, smart hospitals rely on instantaneous communication for tasks such as remote surgery, real-time monitoring of patients, and coordination among medical staff and equipment. OTFS modulation offers benefits in terms of reliability and low latency. Hybrid PAPR reduction algorithms contribute to maintaining these advantages by ensuring that signals are transmitted efficiently and without distortion, even in challenging environments within the hospital premises. Finally, proposed algorithms directly impact the effectiveness of healthcare applications within the smart hospital environment. From remote patient monitoring to real-time video

consultations with specialists, these technologies ensure that critical healthcare services are delivered efficiently and without interruption, ultimately improving patient outcomes and enhancing the overall quality of care.

The structure of the paper is outlined as follows: Section I presents the introduction, Section II details the literature review and contributions made, Section III describes the system model, and Sections IV and V present the simulation results and conclusion of the paper, respectively.

II. Literature Review

OTFS modulation exhibits superior performance compared to the OFDM waveform, particularly under conditions involving high mobility. However, PAPR remains a significant problem in OTFS waveforms. The authors in [13] utilized an auto-encoder and deep-learning-based PAPR reduction approaches. Simulation results demonstrate that the proposed algorithm for PAPR reduction effectively lowers the PAPR in OTFS systems while maintaining a constrained BER. However, the complexity of the algorithm increases owing to its use of complex algorithms. In [14], the authors proposed an airy function-based companding algorithm to minimize large amplitudes of the OTFS. Compared with conventional companding techniques, the proposed algorithm exhibits superior performance, with airy companding demonstrating a marked improvement over the traditional methods. However, the proposed approach does not retain the BER performance of the framework. In [15], the peak power of the OTFS symbol was minimized using exponential and hyperbolic methods. Parameters such as Ber, PAPR, and the attenuation factor were estimated and analyzed. The results of this study reveal that the proposed approach outperforms the conventional companding and clipping methods. In [16], the PAPR of the OTFS, OFDM, and generalized frequency division multiplexing (GFDM) were analyzed and compared. It was observed that the PAPR increased linearly with an increase in the number of subcarriers for OFDM and GFDM. However, in the case of OTFS, the PAPR upsurge coincides with an increase in the number of Doppler domains. The experimental results indicate that orthogonal OTFS modulation achieves a considerable reduction in PAPR compared with OFDM and GFDM. In [17], the authors compared the PAPR performance of OTFS and OFDM and introduced a DFT-spread OTFS waveform under an AWGN and Doppler channel. The authors noted that the DFTS-OTFS achieved a PAPR gain of 2.2 dB and 1.8 dB compared to conventional OFDM and OTFS. In [18], the PAPR of the OTFS was analyzed by applying normalized and companding algorithms. The simulation results revealed that the normalized μ-law outperformed the normalized A-law and conventional companding methods. However, we noticed degradation in the BER performance of the proposed approach. The authors in [19] introduced three PAPR algorithms, namely log root companding, root companding, and the μ-law-based companding algorithm, for the OTFS waveform. The performance of the algorithms was analyzed under different Doppler bins and delays. The experimental results revealed that the proposed PAPR approach outperformed the conventional μ-law method. The authors in [20] proposed a novel wavelet-transform-based SLM and PTS to lower the high peak power of NOMA symbols. The experimental outcomes of the study reveal that the proposed model obtained a PAPR gain of 2 dB and 2.9 dB as compared with the PTS and SLM approaches, respectively. The proposed system, on the other hand, represents an increase in computational complexity. The DSI-based PTS algorithm was used to minimize the PAPR of the NOMA signal [21]. The DSI reassigns the power and reduces the peak value, resulting in the mitigation of high-power variations. The findings of the study demonstrate that the proposed model surpasses the PTS technique, delivering a 3 dB gain in PAPR. In [22], researchers presented a hybrid algorithm designed to decrease the peak power in the NOMA waveform. Experimental evidence suggests that the hybrid algorithm substantially diminishes the PAPR, achieving a gain of 3.2 dB over conventional algorithms. However, the proposed algorithm increases the complexity of the framework. The 4G radio currently utilizes OFDM. The authors of [23] proposed an SLM technique aimed at reducing the high peak amplitude of OFDM symbols. The proposed SLM reduced the original PAPR by 1.6 dB. Researchers introduced a hybrid method that minimizes the peak power of OFDM [24]. The hybrid method achieved a PAPR reduction of 3.2 dB. However, the upsurge was complex, and BER was noted in the proposed model. The contributions of this study are as follows.

1) One of the main contributions is examining how well different hybrid algorithms work by considering factors such as PAPR, BER, and PSD. These include traditional SLM, PTS, A-law, μ-law, and Riemann matrix phase-generation-based SLM and PTS integration with companding approaches. By conducting a comparative analysis of the performance of these methods, we can obtain valuable insights into their ability to effectively reduce the PAPR while maintaining appropriate BER and PSD features.
2) To investigate how OTFS affects the BER performance of different systems using hybrid PAPR reduction techniques, which can increase the throughput of the framework. This offers a thorough understanding of the resistance of the system to BER and PAPR performance.
3) To confirm the integration of different companding approaches with the improved SLM and PTS methods for sub-blocks $s = 4$. This simulation-based validation contributes to verifying the efficacy of the suggested strategies in practical settings and offers insightful information for possible integration with OTFS-based 6G smart hospital systems.
4) The 6G-based smart hospital demands several aspects, such as high spectral access, low power requirements, high through- put, and low latency. The OTFS waveform can be utilized in 6G to fulfil the demands of smart health. The OTFS in 6G enables efficient data transmission in smart hospitals, enhancing communication for real-time monitoring and control. This technology ensures reliable connectivity, reduces interference, and

supports diverse medical applications, ultimately optimizing healthcare delivery, improving patient outcomes, and fostering innovation in the smart-hospital ecosystem. However, an increase in the high PAPR may affect the performance of the OTFS waveform. Hence it is important to designed a PAPTR algorithms which can reduce the PAPR and enhanced the performance of the framework.

III. System Model

An OTFS was implemented using ISFFT and SFFT on the transmitting and receiving sides of the framework. The OTFS symbols are modulated using a Doppler domain, which is transformed into a frequency-time domain using an ISFFT. Accurate assessment of the peak power is crucial for OTFS systems. To achieve this, the OTFS signal was translated into the time domain through the application of a Heisenberg transform [25]. A PAPR reduction technique is employed at the transmitter end to attenuate the high peak power of the OTFS symbol. Subsequently, the signal in the time domain was converted back into the Doppler domain using a Wigner transform at the receiver end of the OTFS system.

The OTFS symbols are represented as [26]

$$Y[k,l] = \frac{1}{kl}\sum_{n=0}^{K-1}\sum_{m=0}^{L-1} y[k,l]e^{i2\pi\left(\frac{kn}{K}-\frac{ml}{L}\right)}. \tag{1}$$

A Heisenberg transform is applied to (1), which results in a time-domain OTFS signal given by [27]

$$s(t) = \sum_{n=0}^{K-1}\sum_{m=0}^{L-1} y[k,l]e^{i2\pi l\Delta f(t-kT)} f_{ty}(t-kT), \tag{2}$$

where f_{ty} represents the transmitted pulse of an OTFS waveform. The discrete time domain of $s(t)$ is acquired using Nyquist sampling, represented as [28]

$$s(v,u_l) = \frac{1}{K}\sum_{k=0}^{K-1} \bar{y}[k] f_{ty}\left([v+u_l-KL]_{KL}\right), \tag{3}$$

where $\bar{y}[k] = \sum_{n=0}^{K-1} y[n,v]e^{j2\pi\frac{kn}{K}}$, $v = 0,1,\cdots,K-1$ and $u = 0,1,\cdots,L-1$. Finally, the PAPR of the OTFS is estimated as

$$PAPR_{\,dB} = 10\log_{10}\left(\frac{\max_{v,u}\left\{|s(v+ul)|^2\right\}}{\frac{1}{KL}\sum_{v=0}^{L-1}\sum_{u=0}^{K-1}\text{Avg}\left\{|s(v+ul)|^2\right\}}\right). \tag{4}$$

It is important to accurately estimate the PAPR. Hence, a CCDF is utilized to determine the PAPR characteristics of the OTFS waveform for larger and smaller thresholds, which are defined as [29]

$$\begin{aligned}\text{Prob}(PAPR > s(v+ul)) =& 1 - \text{Prob}(PAPR \le s(v+ul))\\ =& 1 - \ (1-e^{-s(v+ul)})^t,\end{aligned} \tag{5}$$

$$\begin{aligned}\text{Prob}(PAPR < s(v+ul)) =& F\left(e^{s(v+ul)}\right)^t\\ =& \left(1-e^{-s(v+ul)}\right)^t.\end{aligned} \tag{6}$$

A. SLM

SLM is regarded as one of the most popular PAPR reduction algorithms because it maps the multi-carrier waveform symbol into several unconstrained symbols by weighting the phase rotation elements. Ultimately, a signal that exhibits a reduced PAPR is selected for transmission. Nevertheless, the necessity for side information and the execution of IFFT operations introduce complexity to the process [30].

The steps involved in designing the SLM are as follows [31].

Step 1: The OTFS signals are modulated using a 64-QAM transmission scheme to generate the OTFS symbols given by $s = \{S_0, S_1, \cdots, S_{N-1}\}$.

Step 2: In this step, the OTFS symbols are segmented into sub-blocks of size N subcarriers, given as $s = \sum_{n=0}^{N-1} S_n$.

Step 3: The phase sequence elements give weights to the OTFS sub-blocks (s) $\Phi^p = [\Phi_0^p, \Phi_1^p, \cdots, \Phi_{N-1}^p]^T$, where p is the row element of the particular matrix.

Step 4: A sequence of OTFS sub-blocks is generated, such as

$$S^p = [S_0^p, S_1^p, \cdots, S_{N-1}^p]^T,$$

where $S_n^p = S_n \cdot \Phi_n^p$, for $n = 0,1,\cdots,N-1$.

Step 5: The peak value of the OTFS symbols is determined by applying the IFFT to S^p, which results in $s^p = \text{IFFT}(S^p)$. Finally, the lowest PAPR value of the OTFS symbol from S^p was selected for transmission [32].

SLM can effectively reduce the high PAPR value of the MCW. However, the SLM approach increases the complexity of the framework because of the number of phase-element searches involved in the method [33].

B. PTS

PTS is considered one of the most efficient PAPR algorithms because it enhances the PAPR performance while retaining the BER performance, which results in an increase in the computational complexity of the framework [34].

The input symbols are divided into a number of sub-blocks of size N. An IFFT is applied to each sub-block to estimate the peak amplitude of the signal. The OTFS symbols are multiplied by the phase-rotation elements. To lower the peak power of the OTFS signal s, we select the optimal phase elements [35]

$$s = \sum_{n=1}^{N} \varphi_n S_n. \tag{7}$$

An IFFT is applied to the OTFS signal to estimate the high peak amplitudes of the signal, given as

$$s = \sum_{n=1}^{N} \varphi_n \text{IFFT}(S_n). \tag{8}$$

The (8) can be written as

$$s = \sum_{n=1}^{N} \tilde{\varphi}_n s_n. \tag{9}$$

In (9), the phase elements are selected to minimize the PAPR of an OTFS symbol given by

$$[\tilde{\varphi}_1, \tilde{\varphi}_2, \cdots, \tilde{\varphi}_N] = \arg\min \left(\max \left| \sum_{n=1}^{N} \varphi_n s_n \right|^2 \right). \quad (10)$$

The OTFS signal with minimal PAPR is represented as

$$s = \sum_{n=1}^{N} \tilde{\varphi}_n s_n. \quad (11)$$

It should be noted that the PTS increases the complexity of the framework, as a large number of computations are required to obtain an optimal phase search. Hence, the search for the optimal phase elements is restricted to a smaller number of phase vectors to lower the search complexity of the model.

C. Companding Algorithm

The Companding algorithm significantly reduces the high peak amplitude of the OTFS waveform. The basic principle of the companding method is to compress and decompose the number of subcarriers on the transmitting and receiving sides. A-law and μ-law are complementary algorithms that can be applied to lower the PAPR and spectrum leakage of the OTFS waveform [36].

1) A-law: A-law companding methods reduce the high peak power by compressing the signal on the transmitting side. The A-law expresses the OTFS signal $s(t)$ in the time domain with the compressor parameter C [37]

$$f(s) = \text{sgn}(s) \begin{cases} \frac{C|s|}{1+\ln(C)}, & \text{if } |s| < \frac{1}{C} \\ \frac{1+\ln(C|s|)}{1+\ln(C)}, & \text{if } \frac{1}{C} \le |s| \le 1. \end{cases} \quad (12)$$

2) μ-law: The μlaw companding technique is utilized to decrease the PAPR of the signals, providing a broader dynamic range than that of the A-law technique. However, a notable drawback of this method is the introduction of signal distortion. μ-law gives the OTFS symbol $s(t)$ its value [37]

$$f(s) = \text{sgn}(s) \left\{ \frac{\ln(1+\mu|s|)}{\ln(1+s)} \right\}, \quad -1 \le s \le 1. \quad (13)$$

D. Proposed SLM + Companding Algorithms (SLM+A-law) and (SLM+μ-law)

In this section, we propose a hybrid algorithm to improve the PAPR and PSD to optimal values with minimal complexity and BER, as shown in Fig. 1. Combining SLM with companding is a potent strategy in communication systems to address the challenge of a high PAPR. The SLM intelligently modifies the phase of selected sub-blocks of data to reduce the signal peaks, effectively lowering the PAPR. Concurrently, companding, a compression-expansion technique, reduces the dynamic range of the signal and further mitigates the PAPR. This collaborative approach not only diminishes the PAPR, but also enhances the BER by minimizing signal distortion. In addition, it optimizes the PSD, contributing to the improved spectral efficiency. The synergistic effect results in an enhanced signal quality, lower distortion, and better overall system performance. The Reimann matrix-based SLM is combined with competing algorithms, such as A-law (SLM+A-law) and μ-law (SLM+μ-law). In SLM, OTFS symbols are segmented into a number of sub-blocks. An IFFT was performed to estimate the peak value of an OTFS symbol in the time domain. The Riemann matrix is utilized to produce an optimal phase element factor and reduce complexity by removing the corresponding row and column of a given matrix, as follows [38]

$$m(r,c) = \Big\{ r - 1 \text{if } r \text{ divides } c, \quad (14)$$

$$m(r,c) = \Big\{ -1 \text{for different scenarios.} \quad (15)$$

For instance, let us consider the dimension of the braiding matrix $M \times M$ dimension, and the b_m is optimized by the scaling of $1/M$ represented as $1/M \times b_m$. Let us consider an OTFS signal in the time domain, represented as [39]

$$s = [S_0, S_1, \cdots, S_{N-1}]^T. \quad (16)$$

The OTFS symbols are segmented into a number of subcarriers, $n = 0, 1, \cdots, N-1$. The OTFS symbols are weighted with the phase elements generated by the b_m given as follows

$$b^p = \left[b_0^p, b_1^p, \cdots, b_{N-1}^p \right]^T. \quad (17)$$

The OTFS symbols are weighted with the phase element given by

$$S_N^p = b_{mN}^p \; S_N. \quad (18)$$

The amplitude of the S_N^p is estimated by using IFFT transform, represented as

$$s_N^p(t) = \text{IFFT}\left(S_N^p\right), \quad (19)$$

$$s_N^p(t) = b_{mN}^p \cdot \text{IFFT}\left(S_N\right). \quad (20)$$

Finally, the PAPR reduction is achieved by selecting the symbol with the lowest PAPR value

$$b_{m1}^p, b_{m2}^p, \cdots, b_{mN}^p = \arg\min \left(\max \left| \sum_{n=1}^{N} b_{mN}^p s_N^p(t) \right|^2 \right). \quad (21)$$

Further, to reduce the number of papers and improve the spectrum leakage, competing algorithms such as A-law and μ-law are applied to the OTFS signal. The PTS + A law is expressed as follows

$$f\left(s_N^p(t)\right)_{\text{A-law}} = \text{sgn}\left(s_N^p(t)\right) \begin{cases} \frac{C|s_N^p(t)|}{1+\ln(C)}, & \text{if } |s_N^p(t)| \le \frac{1}{C} \\ \frac{1+\ln(C|s_N^p(t)|)}{1+\ln(C)}, & \text{if } \frac{1}{C} \le |s_N^p(t)| \le 1. \end{cases} \quad (22)$$

The PTS +μ-law is represented as

$$f\left(s_N^p(t)\right)_{\mu\text{-law}} = \text{sgn}\left(s_N^p(t)\right) \left\{ \frac{\ln\left(1+\mu|s_N^p(t)|\right)}{\ln(1+s_N^p(t))}, \quad -1 \le s_N^p(t) \le 1 \right. . \quad (23)$$

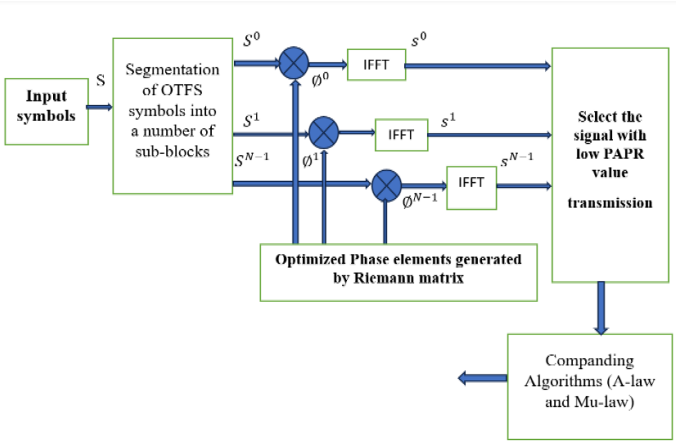

Fig. 1. Proposed SLM+Companding methods.

E. Proposed PTS + Companding Algorithms (PTS+A-law) and (PTS+ μ-law)

Integrating PTS with companding is an effective strategy in communication systems to alleviate the detrimental impact of a high PAPR. The PTS strategically redistributes signal peaks, lowering the PAPR and minimizing signal distortion. Companding, a compression-expansion process, further aids in reducing the dynamic range of the signal. This tandem approach not only curtails the PAPR but also enhances the BER by mitigating signal distortion and improving the PSD by optimizing the spectral efficiency. Overall, this synergistic solution results in more efficient use of the available bandwidth, ensuring better signal quality and system performance.

In this section, we propose a modified PTS approach in which the phase elements are optimized as follows

$$s = \left[S_0, S_1, \cdots, S_{N-1}\right]^T. \tag{24}$$

Applying IFFT in (24) results in

$$s(t) = \text{IFFT}\left(S\right), \tag{25}$$

$$s(t) = \left[s_0, s_1, \cdots, s_{N-1}\right]^T. \tag{26}$$

The optimized phase element vectors are generated by a Riemann matrix, which lowers the PAPR by multiplying by the OTFS symbol s(t). The phase sequence of the Riemann matrix is given by [40]

$$R_m(r,c) = \begin{cases} r-1, & \text{for } \frac{r}{c} \\ -1, & \text{else} \end{cases}. \tag{27}$$

where r and c represent the row and column, respectively, and R_m. Let us consider that the dimensions of R_m is given by $N \times N$ and the elements optimized in R_m are scaled by a factor of $1/N$ as $1/N \times R_m$. The element in the corresponding P-th row is a component of P or -1, $1 \leq P \leq N$. Hence, if the value of R_m is 1, then there is a phase shift of the signal, and the value of p results in an amplitude change of the OTFS signal [38]. The multiplication of an OTFS symbol with the R_m phase elements is given by

$$s(t) = \sum_{n=1}^{N} \overline{R_{mn}} S_n. \tag{28}$$

The PAPR is minimized by selecting the optimal value of phase elements

$$\left[\overline{R_{m1}}, \overline{R_{m2}}, \cdots, \overline{R_{mN}}\right] = \arg\min\left(\max\left|\sum_{n=1}^{N} \overline{R_{mn}} S_n\right|^2\right). \tag{29}$$

To further enhance the PAPR performance with optimal BER and PSD, companding methods were applied after the PTS. The PTS +A-law is given as

$$f\left(s(t)\right)_{\text{A-law}} = \text{sgn}\left(s_N^p(t)\right) \begin{cases} \frac{C|s(t)|}{1+\ln(C)}, & \text{if } |s(t)| < \frac{1}{C} \\ \frac{1+\ln(C|s(t)|)}{1+\ln(C)}, & \text{if } \frac{1}{C} \leq |s(t)| \leq 1 \end{cases}. \tag{30}$$

The PTS +μ-law is represented as

$$f\left(s(t)\right)_{\mu\text{-law}} = \text{sgn}\left(s(t)\right) \left\{ \frac{\ln(1+\mu|s(t)|)}{\ln(1+s(t))}, \quad \text{if } -1 \leq s(t) \leq 1 \right. . \tag{31}$$

IV. Simulation Results

This section is dedicated to the evaluation and comparison of the performance of the traditional and newly proposed PAPR reduction algorithms with respect to the OTFS waveform. Simulations were performed using MATLAB 2019. We utilized parameters such as $N = 256$ subcarriers, 64-QAM, 256-FFT, 20000 symbols, and sub-blocks (2 and 4) with Rician and Rayleigh channels. In Fig. 2, we perform PAPR analysis of multi-carrier waveforms such as OTFS, NOMA, FBMC, and OFDM under a Rayleigh channel without applying PAPR algorithms. It is seen that the PAPR values of 9.2 dB (OTFS), 10.6 dB (NOMA), 11.3 dB (FBMC), and 12 dB (OFDM) are obtained at the CCDF of 10^{-3}.

It is determined that OTFS modulation exhibits a PAPR gain of 1.4 dB, 2.1 dB, and 2.8 dB over other modern waveforms

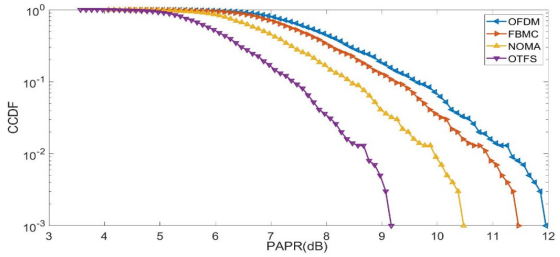

Fig. 2. PAPR analysis of advanced waveform under Rayleigh channel.

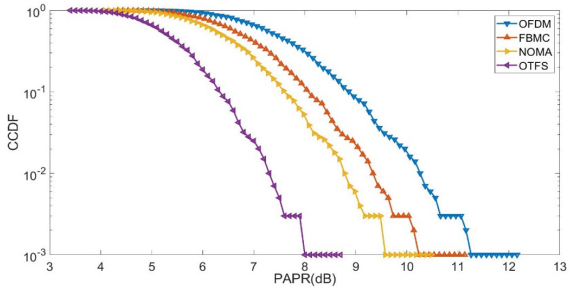

Fig. 3. PAPR analysis of advanced waveform under Rician channel.

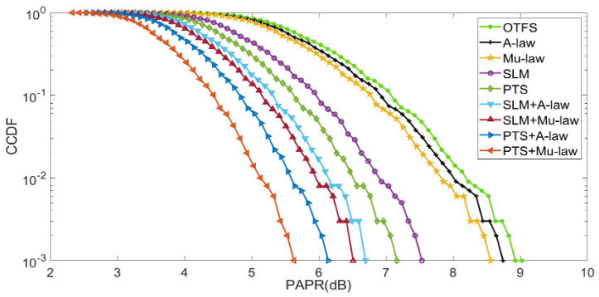

Fig. 4. PAPR analysis of OTFS under Rayleigh channel.

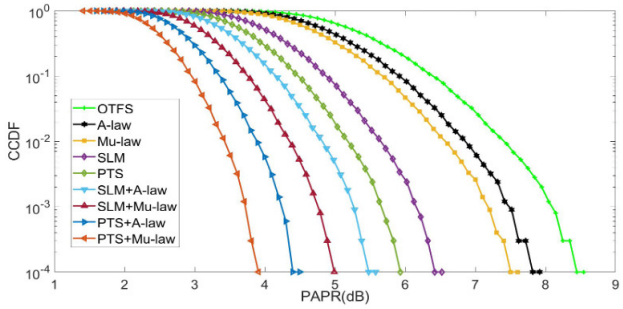

Fig. 5. PAPR analysis of OTFS under Rician channel.

such as NOMA, FBMC, and OFDM respectively. The superior PAPR performance of the OTFS in Rayleigh channels is attributed to its distinctive time-frequency processing capabilities, which effectively minimize amplitude fluctuations and bolster signal resilience. This enhances communication dependability, particularly in environments with challenging fading characteristics.

Fig. 3 illustrates the PAPR analysis of various advanced waveforms in a Rician channel, excluding the application of PAPR reduction techniques. At a CCDF of 10^{-3}, the PAPRs for OTFS, NOMA, FBMC, and OFDM are recorded at 8.2 dB, 9.7 dB, 10.2 dB, and 11.2 dB respectively. It is observed that multi-carrier waveforms exhibit improved PAPR performance in Rician channels compared with Rayleigh channels. The superior PAPR performance of the OTFS under Rician conditions can be attributed to the adept handling of multipath scenarios. OTFS not only proves to be more reliable than other contemporary waveforms under Rician channel conditions but also demonstrates increased robustness by utilizing its time-frequency processing to effectively mitigate variations in amplitude.

In Fig. 4, the conventional and proposed hybrid algorithms under a Rayleigh channel were applied to the OTFS waveform. The main objective is to determine the PAPR and reduce it to an optimal value. At the CCDF of 10^{-3}, the PAPR values of 8.8 dB, 8.6 dB, 7.7 dB, 7.2 dB, 6.8 dB, 6.6 dB, 6.1 dB, and 5.8 dB are obtained by the A-law, μ-law, SLM, PTS, SLM+A-law, SLM+μ-law, PTS+A-law, and PTS+μ-law, respectively. It was observed that the hybrid algorithms outperformed the conventional methods. However, the proposed PTS+μ-law obtained significant PAPR minimization compared with contemporary PAPR methods. The hybrid algorithms reduced the PAPR to 3 dB compared with the OTFS waveform (8.8 dB). The combination of SLM, PTS, and complementing algorithms enhances the PAPR performance in OTFS. SLM reduces PAPR by applying phase sequences, optimizes phase factors, reduces peaks and compresses the signal, reduces dynamic range, and further mitigates peaks, collectively improving the OTFS communication efficiency and reliability.

The PAPR of the OTFS waveform was estimated under a Rician channel for the proposed hybrid and conventional PAPR algorithms, as shown in Fig. 5. The original PAPR of the OTFS is 8.6 dB at the CCDF of 10^{-3}, which is reduced to 7.9 dB by A-law, 7.7 dB by μ-law, 6.8 dB by SLM, 5.9 dB by PTS, 5.6 dB by SLM+A-law, 5 dB by SLM+μ-law, 4.5 dB by PTS+A-law, and 3.8 dB by PTS+μ-law, respectively. Hence, it is noted that the PTS+μ-law obtained a gain of 0.7 dB to 4 dB as compared with the other proposed methods.

The PAPR performance of the conventional and hybrid algorithms with sub-blocks ($s = 4$) under a Rayleigh channel was estimated, as shown in Fig. 6. The PAPR of the OTFS was 9.2 dB at a CCDF of 10^{-3}. The PAPR of the OTFS is reduced to 6.2 dB by SLM ($s = 4$), 5.6 dB by PTS ($s = 2$), and 5.2 dB by SLM+A-law ($s = 4$). 4.5 dB SLM+μ-law ($s = 4$), 4.1 dB PTS+A-law ($s = 2$), and 3.2 dB PTS+μ-law ($s = 4$), respectively. It is concluded that the most favorable PAPR is achieved by augmenting the number of sub-blocks in the transmission scheme, with the proposed PTS combined with μ-law companding outshining the other PAPR reduction schemes presented in this work. An increase in the size of the sub-blocks within the hybrid algorithms amplifies the PAPR performance in the Rayleigh channels. The utilization of larger sub-blocks enhances signal diversity, which counters the deleterious effects of fading and contributes to a more effective peak reduction. This, in turn, leads to an

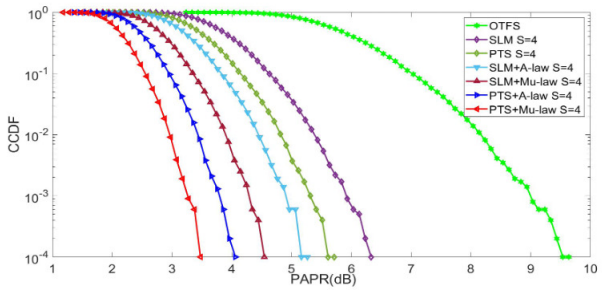

Fig. 6. PAPR analysis of OTFS under Rayleigh channel for sub-blocks (s=4).

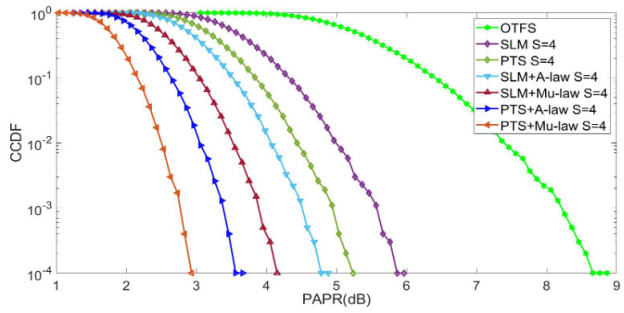

Fig. 7. PAPR analysis of OTFS under Rician channel for sub-blocks (s=4).

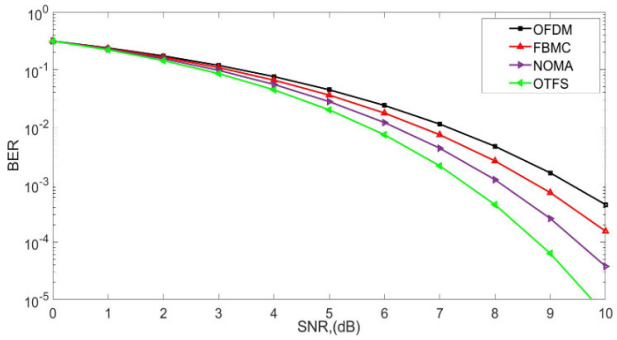

Fig. 8. BER analysis of advanced waveforms under Rician channel.

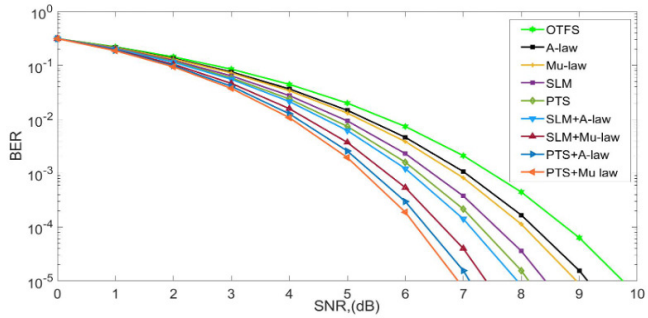

Fig. 9. BER analysis of an OTFS waveform under Rician channel.

enhancement in the overall PAPR profile of the system.

The PAPR curves of the OTFS waveform under a Rician channel for different subblocks ($s = 2$ and 4) are shown in Fig. 7. At the CCDF of 10^{-3}, the PAPR of the OTFS signal is reduced to 5.9 dB (SLM $s = 4$), 5.2 dB (PTS $s = 4$), 4.8 dB (SLM+A-law $s = 4$), 4.2 dB (SLM+μ-law $s = 2$), 3.6 dB (PTS+A-law $s = 4$), and 2.9 dB (PTS+μ-law), respectively. The results show that the proposed PTS+μ-law outperforms contemporary PAPR methods. Furthermore, it is concluded that expanding the sub-block sizes in the proposed hybrid algorithms within a Rician channel enhances the PAPR performance. Larger sub-blocks contribute to increased signal diversity, mitigate Rician fading effects, and improve the peak reduction capabilities. This leads to superior PAPR characteristics and overall transmission efficiency in the Rician channels.

Several PAPR algorithms can effectively reduce the high peak power of multi-carrier waveforms without compromising the BER performance. Hence, it is important to retain the throughput performance of the framework while minimizing the PAPR value of advanced waveforms. Therefore, it is important to analyze the throughput performance of the proposed algorithms using the OTFS waveform. In Fig. 8, the BER curves of the advanced waveform are determined using a Rician channel. The BER of 10^{-3} is acquired at the SNR of 7.5 dB, 8.3 dB, 8.7 dB, and 9.4 dB by the OTFS, NOMA, FBMC, and OFDM waveforms. Hence, OTFS without the PAPR reduction obtained an SNR gain of 0.8 dB, 1.2 dB, and 1.9 dB as compared with the existing waveforms (NOMA, FBMC, and OFDM).

The BER of an OTFS under a Rician channel is estimated using the conventional and proposed hybrid schemes, as shown in Fig. 9. The main focus was to analyze whether the BER performance was retained by the proposed algorithms. At the BER, the SNRs of 5.1 dB, 5.5 dB, 5.8 dB, 6.1 dB, 6.3 dB, 6.5 dB, 7 dB, and 7.2 dB are obtained by the A-law, μ-law, SLM, PTS, ALM+A-law, SLM+μ-law, PTS+A-law, and PTS+μ PAPR schemes. The PTS+μ-law obtained an efficient throughput compared with existing methods. Hence, it is concluded that the proposed hybrid algorithms retain their BER performance while reducing the PAPR of the signal.

Fig. 10 shows the BER performance of an OTFS waveform under the Rician channel for subblocks ($s = 4$). For sub-blocks $s = 4$, the BER of 10^{-3} is achieved at the SNR of 6.1 dB (SLM $s = 4$), 5.6 dB (PTS $s = 4$), 5.3 dB (SLM+A-law $s = 4$), 4.8 dB (SLM+μ-law $s = 4$), 4.2 dB (PTS+A-law $s = 4$), and 3.7 dB (PTS+μ-law $s = 4$), respectively. It is seen that the hybrid algorithms outperform the conventional algorithms and have superior throughput performance. Hence, it is concluded that an increase in sub-blocks can efficiently retain and improve the BER performance without compromising the PAPR performance.

The enhancement of PSD in 6G-based smart hospitals optimizes wireless communication, boosts data transfer rates, and accommodates diverse medical applications. This improvement ensures efficient spectrum utilization; minimizes interference; and supports a robust, high-capacity network, ultimately advancing the quality, speed, and reliability of healthcare data transmission.

In the proposed article, SLM combined with μ-law and A-law companding techniques outperform original OTFS due to their ability to reduce PAPR without compromising BER

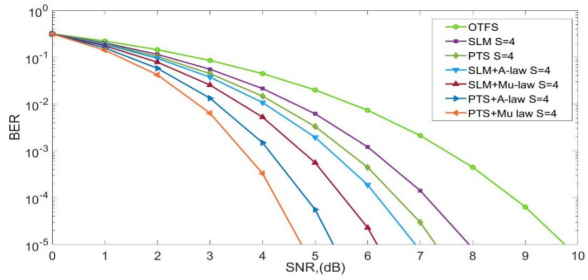

Fig. 10. BER analysis of an OTFS waveform under Rician channel for sub-block (s= 4).

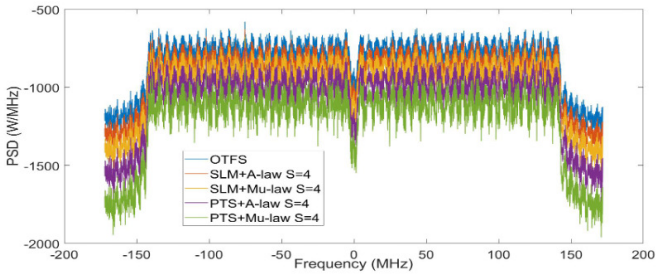

Fig. 11. PSD performance of OTFS under Rician channel (s=4).

performance. SLM optimally redistributes the signal constellation, mitigating high peak amplitudes, thereby reducing nonlinear distortion effects. Meanwhile, μ-law and A-law companding introduce controlled nonlinear transformations, effectively compressing dynamic range and enhancing signal robustness against channel impairments. Consequently, while PAPR is reduced, BER performance improves, demonstrating the synergy between PAPR reduction techniques and error mitigation strategies in improving overall system performance.

In Fig. 11, we analyzed the performance of the conventional and proposed hybrid algorithms when applied to the OTFS waveform. It can be seen that the hybrid algorithms obtained a PSD value of -1390 (SLM+A-law $s = 4$), -1436 (SLM+μ-law $s = 4$), -1618 (PTS+A-law $s = 4$), and -1881 dB (PTS+μ-law $s = 4$), respectively, as compared with the OTFS (-1320). Hence, increasing the sub-block size to four in the hybrid enhances the PSD. This expansion results in a more effective distribution of transmitted power, thereby reducing spectral regrowth. Larger subblocks mitigate signal distortions, minimize out-of-band emissions, and improve the overall PSD. Consequently, this leads to a more efficient and spectrally compliant communication system with enhanced power spectral density.

The enhancement of PSD in 6G-based smart hospitals optimizes wireless communication, boosts data transfer rates, and accommodates diverse medical applications. This improvement ensures efficient spectrum utilization; minimizes interference; and supports a robust, high-capacity network, ultimately advancing the quality, speed, and reliability of healthcare data transmission. In Fig. 12, we analyzed the spectral access performance of the advanced waveforms for a 6G-based smart hospital under a Rician channel. The PSD values obtained by PTS+μ-law, PTS+A-law, SLM+μ-law, and SLM+A-law are -1320, -1070,-830, and -670 dBm/Hz, respectively. PTS+μ-law obtained a significant PSD gain of $-230, -470$, and -630 dBm/Hz as compared with contemporary algorithms and successfully reduced out-of-band radiation as compared with contemporary waveforms. Hence, the PTS+μ-law in OTFS can efficiently utilize the spectrum and accommodate a greater number of pieces of information, which will be ideal for a 6G-based smart hospital.

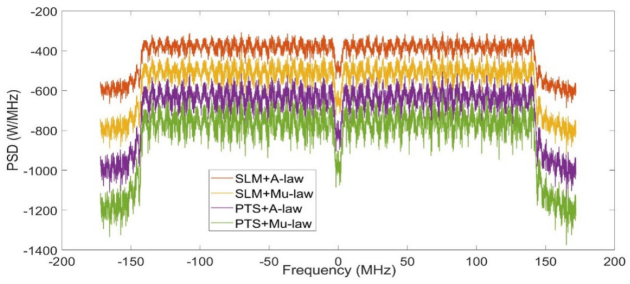

Fig. 12. PSD anlaysis of proposed hybrid algorithms.

A. Complexity Analysis

SLM is a PAPR reduction technique that introduces complexity owing to the exhaustive search for optimal phase sequences. The computational load increases significantly as it explores a vast solution space to minimize the PAPR, striking a balance between effectiveness and computational efficiency. The PTS complicates the implementation by shaping the temporal profile of the transmitted signals. The design of optimal pulse sequences involves intricate considerations of the filter characteristics, requiring a delicate balance between complexity, bandwidth efficiency, and PAPR reduction performance. Combining SLM with Companding introduces synchronization challenges between the spatial and amplitude compression-expansion processes. This complexity arises from the need for sophisticated algorithms to effectively coordinate and calibrate these two operations. PTS combined with companding adds further intricacies by simultaneously optimizing the temporal and amplitude aspects. Coordinating pulse shaping and companding functions requires intricate trade-offs to achieve PAPR reduction without compromising signal quality, adding complexity to the design and implementation of these algorithms. Hence, the complexity of these PAPR reduction methods stems from the intricate trade-offs between computational load, synchronization, and optimization, highlighting the challenges in achieving an effective PAPR reduction while maintaining system efficiency. Table I lists the complexity of the proposed method.

The combination of SLM, PTS, and companding techniques offers advantages over DFT spread OTFS signals in PAPR reduction and overall system performance. SLM and PTS efficiently redistribute signal energy, mitigating high peak amplitudes and reducing PAPR without significant signal distortion. Companding techniques, such as μ-law or A-law companding, further compress the dynamic range of the signal, enhancing robustness against nonlinear distortion effects. In contrast, DFT spread OTFS signals lack these specific PAPR

TABLE I
COMPLEXITY.

No.	PAPR reduction algorithms	Complexity
1.	SLM	$C = O(K.M^N E)$, where K is the computational effort per candidate phase sequence, M^N represents the search space size, which accounts for exploring different phase sequences for each sub-block, and E is the computational effort involved in evaluating the PAPR for each candidate sequence.
2.	A-law	$C = O(K_{\text{A-law}}N)$, where $K_{\text{A-law}}$ is a constant factor representing the computational effort per sample, and N is the number of samples in the OTFS signal.
3.	μ-law	$C = O(K_{\mu\text{-law}}N)$, where $K_{\mu\text{-law}}$ is a constant factor representing the computational effort per sample, and N is the number of samples in the OTFS signal.
4.	PTS	$C = O(N^K \cdot (\log_2 M)^N E)$
5.	SLM+ companding	$C = O(K.M^N E) \cdot (K_{\text{A-law}}N)$
6.	PTS+ companding	$C = O(N^K \cdot (\log_2 M)^N E) \cdot (K_{\text{A-law}}N)$

reduction mechanisms, leading to higher PAPR values and increased susceptibility to nonlinear distortion. Consequently, the combined SLM, PTS, and companding approach ensures lower PAPR levels, improved signal quality, and enhanced spectral efficiency, making it preferable for reliable and efficient communication systems, especially in challenging environments. See Table II for a comparison of the proposed article with the published work.

B. Comparative Analysis of the proposed hybrid methods

In Table III, we have compared and analysed the proposed hybrid methods for an OTFS waveform with Rayleigh and Rician channel.

The PAPR performance of the hybrid PAPR algorithms are analyzed and compared with conventional methods. It is seen that the proposed methods obtained an optimal performance in Rician channel as compared with the Rayleigh channel. The graph reveals that the proposed PTS+μ-law obtained a superior performance as compared with the contemporary waveforms (5.8 dB in Rayleigh and 3.8 dB in Rician channel). The PAPR performance of the hybrid PAPR algorithms with sub-blocks ($s = 4$) for the Rayleigh and Rician channel is estimated. It is seen that the proposed methods obtained an optimal performance than Rayleigh channel just by increasing the number of sub-blocks($s = 4$) in Rician channel as compared with the Rayleigh channel. The graph reveals that the proposed PTS+μ-law obtained a superior performance as compared with the contemporary waveforms (3.2 dB in Rayleigh and 2.9 dB in Rician channel). The BER performance of the hybrid algorithms with and without sub-blocks ($s = 4$) is analyzed. It is seen that the hybrid method with sub-blocks ($s = 4$) outperforms the contemporary methods. It is also revealed that the PTS+μ-law ($s = 4$) obtained an efficient BER performance of 10^{-3} at the SNR of 3.7 dB. The PSD performance of the proposed hybrid algorithms for Rician channel is estimated. It is noted that the proposed algorithm significantly lowers the sidelobe to enhance the spectral access of the framework. It is concluded that the PTS+μ-law ($s = 4$) outperforms the contemporary algorithms by obtaining the PSD of -1881.

The PAPR reduction in OTFS modulation contributes to the advancement of smart hospital technology by improving wireless communication reliability, extending device battery life, enabling remote healthcare services, and enhancing overall patient care and operational. Some application related to PAPR reduction with smart health care are given below:

1) PAPR reduction enhances the reliability and efficiency of wireless communication channels between wearable health monitoring devices and hospital systems. This ensures accurate and timely transmission of patient data, facilitating remote monitoring and enabling healthcare providers to make informed decisions promptly.
2) Implantable sensors and devices benefit from PAPR reduction in OTFS signals, as it enables efficient and reliable communication with external monitoring systems. Reduced PAPR helps extend battery life in these devices, minimizing the need for frequent replacements and improving patient comfort.
3) PAPR reduction supports robust and low-latency communication links essential for telemedicine applications within smart hospitals. By reducing signal distortion and interference, OTFS modulation with lower PAPR ensures high-quality audio and video transmission during remote consultations, enhancing the patient experience and enabling effective virtual healthcare delivery.

V. CONCLUSION

The 6G-based smart hospital demands several aspects, such as high spectral access, low power requirements, high throughput, and low latency. The OTFS waveform can be utilized in 6G to fulfill the demands of smart health. The OTFS in 6G enables efficient data transmission in smart hospitals, enhancing communication for real-time monitoring and control. This technology ensures reliable connectivity, reduces interference, and supports diverse medical applications, ultimately optimizing healthcare delivery, improving patient outcomes, and fostering innovation in the smart-hospital ecosystem. However, an increase in the high PAPR may affect the performance of the OTFS waveform. This article presents a hybrid algorithm that combines SLM, PTS, and companding techniques within Rayleigh-Rician channels. Conventional SLM and PTS are enhanced through phase element optimization via the Riemann matrix coupled with A-law and μ-law integration, reducing the PAPR and BER while improving the PSD in the radio system. Hybrid algorithms, such as SLM+A-law, SLM+μ-law, PTS+A-law, and PTS+μ-law, demonstrated enhanced performance over traditional methods. Furthermore, the proposed algorithms were analyzed by increasing the number of sub-blocks ($s = 4$). Increasing the sub-block size improves PAPR by providing more possibilities for phase weighting. A larger sub-block allows for finer granularity in adjusting the phases of the individual sub-blocks, enabling a better cancellation effect

TABLE II
COMPARISON WITH EXISTING WORK.

Ref.	Remarks
[41]	System model: DL algorithms 1) The article presents experimental results and performance evaluations to demonstrate the effectiveness and efficiency of the proposed algorithm in reducing PAPR in OFDM systems. 2) The article has not comprehensively addressed all relevant performance metrics such as computational complexity, spectral efficiency, and SLM with number of sub-blocks. 3) The proposed article provides no comparison between other waveforms such as FBMC, NOMA, and OTFS. Simulation parameters: • BER and PAPR analysis is performed • Waveform: OFDM • Channel: Rayleigh channel
[42]	System Model: DL-autoencoder 1) The article provides experimental validation of the proposed method, which enhances the credibility of the research findings. This includes simulations or real-world implementations, validating the effectiveness of the proposed approach. 2) The article has not discussed the performance of the parameters in Rician channel. 3) The article has not discussed the computational requirements and PSD and comparison with other contemporary algorithms. Simulation parameters: • PAPR is implemented • Waveform: OFDM • Channel: Rayleigh channel
[43]	System model: ANN based SLM 1) The article may lack a comprehensive comparison with existing PAPR reduction techniques in OFDM waveform. Without a thorough comparison with other advanced waveform, it could be challenging to assess the effectiveness of the proposed algorithm against state-of-the-art approaches. 2) The SLM is integrated with Neural network algorithms but the article does not provide the intricacy of the framework. 3) The sub-blocks analysis is not performed under different condition and PSD of the waveform is not discussed in the presented paper. Simulation parameters: • PAPR and BER is implemented • Waveform: OFDM • Channel: Rayleigh channel
[44]	System model: SLM with auto encoder 1) Lack of comparative analysis with alternative PAPR reduction techniques, hindering assessment of its effectiveness relative to existing methods. 2) Insufficient discussion on the robustness and generalization of the proposed scheme across diverse channel conditions and system configurations. Simulation parameters: • PAPR and BER is implemented • Waveform: OFDM • Channel: Rayleigh channel
[45]	System model: DL based Tone Reservation 1) Tone reservation method based deep learning for PAPR reduction may face challenges in handling nonlinear distortions, complex channel conditions, and high computational complexity. 2) Additionally, it may require substantial labelled training data, limiting its applicability in scenarios with limited datasets or varying channel characteristics. Simulation parameters: • PAPR and BER are implemented • Waveform: OFDM • Channel: Rayleigh channel
Proposed algorithm	System model: SLM+A-law, SLM+μ-law, PTS+A-law, PTS+μ-law with $s = 4$ 1) SLM exploits diversity gains and computational efficiency, reducing PAPR effectively. Additionally, μ-law and A-law companding introduce nonlinearity, aiding in PAPR reduction with simplicity and low complexity. 2) Unlike deep learning, these methods require less training overhead, are robust to channel variations, and offer better performance in scenarios with limited labeled data or computational resources. 3) BER and PAPR analysis of advanced waveforms such as OFDM, FBMC, and NOMA with OTFS are performed. 4) The complexity analysis is provided in the proposed work. 5) The proposed algorithms are compared with A-law, μ-law, SLM and PTS in Rician and Rayleigh channel considering the sub-blocks analysis. Simulation parameters: • PAPR, BER, and PSD are implemented • Waveform: OFDM, FBMC, NOMA, and OTFS • Channel: Rician and Rayleigh

TABLE III
COMPARATIVE ANALYSIS OF PROPOSED HYBRID ALGORITHM.

PAPR algorithms	**PAPR (dB) Rayleigh channel**	**PAPR (dB) Rician channel**	**BER of 10^{-3} SNR (dB) Rician channel**	**PSD value in Rician channel**
SLM+A-law	6.8	5.6	6.3	-670
SLM-μ-law	6.6	5.0	6.5	-830
PTS+A-law	6.1	4.5	7.0	-1070
PTS+μ-law	5.8	3.8	7.2	-1320
SLM+A-law (s = 4)	5.2	4.8	5.3	-1390
SLM+μ-law (s = 4)	4.5	4.2	4.8	-1436
PTS+A-law (s = 4)	4.1	3.6	4.2	-1618
PTS+μ-law (s = 4)	3.2	2.9	3.7	-1881

and reducing amplitude variations. This enhancement helps minimize the signal peaks, enhances the overall signal quality, and reduces the PAPR in communication systems. In conclusion, the proposed algorithms were found to significantly improve battery longevity and spectral efficiency, which in turn enhances the dependability of wireless communications. This advancement ensures that medical devices maintain robust and efficient connectivity, which is essential for the uninterrupted transmission of data crucial for patient monitoring and other healthcare applications. Efforts to minimize PAPR for OTFS-based 6G smart hospital systems will focus on the refinement of algorithms and the investigation of adaptive strategies to guarantee both efficient and dependable wireless communication in healthcare settings.

REFERENCES

[1] C. de Alwis, Q.-V. Pham, and M. Liyanage, *6G Radio Access Networks*. Wiley-IEEE Press, 2023, pp. 99–114.

[2] H. Kwon *et al.*, "Review of smart hospital services in real healthcare environments," *Healthcare Informatics Research*, vol. 28, no. 1, pp. 3–15, 2022.

[3] A. Kumar, M. A. Albreem, M. Gupta, M. H. Alsharif, and S. Kim, "Future 5G network based smart hospitals: Hybrid detection technique for latency improvement," *IEEE Access*, vol. 8, pp. 153 240–153 249, 2020.

[4] O. Rajaei, S. R. Khayami, and M. S. Rezaei, "Smart hospital definition: Academic and industrial perspective," *Int. J. Medical Inform.*, p. 105304, 2023.

[5] B. Ç. Uslu, E. Okay, and E. Dursun, "Analysis of factors affecting IoT-based smart hospital design," *J. Cloud Comput.*, vol. 9, no. 1, p. 67, Nov 2020.

[6] C. de Alwis, Q.-V. Pham, and M. Liyanage, *6G for Healthcare*. Wiley-IEEE Press, 2023, pp. 189–196.

[7] A. Kumar, R. Dhanagopal, M. A. Albreem, and D.-N. Le, "A comprehensive study on the role of advanced technologies in 5G based smart hospital," *Alexandria Eng. J.*, vol. 60, no. 6, pp. 5527–5536, 2021.

[8] W. Yuan *et al.*, "New delay doppler communication paradigm in 6G era: A survey of orthogonal time frequency space (OTFS)," *China Commun.*, vol. 20, no. 6, pp. 1–25, 2023.

[9] Z. ZHANG, H. LIU, Q. WANG, and P. FAN, "A survey on low complexity detectors for OTFS systems," *ZTE Commun.*, vol. 19, no. 4, pp. 3–15, 2022.

[10] A. Kumar, N. Gour, S. K. Yadav, N. Gaur, and H. Sharma, "A comparative PAPR, ber, and psd for optical NOMA communication framework," *Optical Quantum Electron.*, vol. 55, no. 10, p. 890, 2023.

[11] A. Kumar *et al.*, "Evaluation of 5G techniques affecting the deployment of smart hospital infrastructure: Understanding 5G, AI and IoT role in smart hospital," *Alexandria Eng. J.*, vol. 83, pp. 335–354, 2023.

[12] A. Kumar, S. Chakravarty, A. K, and M. Sharma, *5G-Based Smart Hospitals and Healthcare Systems: Evaluation, Integration, and Deployment*, 1st ed., A. Kumar, S. Chakravarty, A. K, and M. Sharma, Eds. CRC Press, 2023. [Online]. Available: https://doi.org/10.1201/9781003403678

[13] M. Liu, M.-M. Zhao, M. Lei, and M.-J. Zhao, "Autoencoder based PAPR reduction for OTFS modulation," in *Proc. IEEE VTC2021-Fall*, 2021.

[14] H. Bitra, C. Anusha, and N. C. Pradhan, "Reduction of PAPR in OTFS signal using airy special function," *J. Optical Commun.*, no. 0, 2023.

[15] H. Bitra, P. Ponnusamy, S. Chintagunta, and S. Pragadeshwaran, "Nonlinear companding transforms for reducing the PAPR of OTFS signal," *Physical Commun.*, vol. 53, p. 101729, 2022.

[16] G. Surabhi, R. M. Augustine, and A. Chockalingam, "Peak-to-average power ratio of OTFS modulation," *IEEE Commun. Lett.*, vol. 23, no. 6, pp. 999–1002, 2019.

[17] M. N. Hossain, Y. Sugiura, T. Shimamura, and H.-G. Ryu, "DFT-spread OTFS communication system with the reductions of PAPR and nonlinear degradation," *Wireless Personal Commun.*, vol. 115, no. 3, pp. 2211–2228, 2020.

[18] H. Bitra, P. Ponnusamy, and S. Chintagunta, "Reduction of PAPR in OTFS using normalized μ-law and a-law companding transform," *Internet Technol. Lett.*, vol. 5, no. 3, p. e344, 2022.

[19] H. Bitra, P. Ponnusamy, and S. Chintagunta, "Reduction of PAPR in OTFS using rooting companding techniques," *Int. J. Electron. Lett.*, pp. 1–12, 2022.

[20] M. K. Sharma and A. Kumar, "PAPR reduction in NOMA by using hybrid algorithms." *Computers, Materials & Continua*, vol. 69, no. 1, 2021.

[21] R. Sayyari, J. Pourrostam, and H. Ahmadi, "A low complexity pts-based PAPR reduction method for the downlink of OFDM-NOMA systems," in *Proc. IEEE WCNC*, 2022.

[22] A. Kumar, N. Gour, H. Sharma, and R. Pareek, "A hybrid technique for the PAPR reduction of NOMA waveform," *Int. J. Commun. Syst.*, vol. 36, no. 4, p. e5412, 2023.

[23] Y.-h. Xu, J.-Y. Oh, Z.-h. Sun, and M.-S. Lim, "A novel method for PAPR reduction of the OFDM signal using nonlinear scaling and fm," *Frontiers of Information Technology & Electronic Engineering*, vol. 20, no. 11, pp. 1587–1594, 2019.

[24] A. Kumar, "PAPR reduction of fbmc using hybrid and k-hybrid techniques," *Radioelectronics and Communications Systems*, vol. 62, no. 10, pp. 501–509, 2019. [Online]. Available: https://doi.org/10.3103/S0735272719100029

[25] P. Gu, L. Guo, S. Jin, G. Liu, and J. Zou, "Otfs-IM modulation based on four-dimensional spherical code in air-to-ground communication," *Drones*, vol. 7, no. 10, p. 631, 2023.

[26] H. Shang *et al.*, "Otfs modulation and PAPR reduction for IoT-railways," *China Commun.*, vol. 20, no. 1, pp. 102–113, 2023.

[27] R. Hadani *et al.*, "Orthogonal time frequency space modulation," in *Proc. IEEE WCNC*, 2017.

[28] Z. Wei *et al.*, "Orthogonal time-frequency space modulation: A promising next-generation waveform," *IEEE Wireless Commun.*, vol. 28, no. 4, pp. 136–144, 2021.

[29] P. Raviteja, K. T. Phan, and Y. Hong, "Embedded pilot-aided channel estimation for OTFS in delay–doppler channels," *IEEE Trans. Veh. Technol.*, vol. 68, no. 5, pp. 4906–4917, 2019.

[30] A. Kumar *et al.*, "PAPR reduction using SLM-PTS-CT hybrid PAPR method for optical NOMA waveform," *Heliyon*, vol. 9, no. 10, 2023.

[31] M. Mounir, M. I. Youssef, and A. M. Aboshosha, "Low-complexity selective mapping technique for PAPR reduction in downlink power domain OFDM-NOMA," *EURASIP J. Advances Signal Process.*, vol. 2023, no. 1, p. 10, 2023.

[32] A. Kumar and M. Gupta, "A comprehensive study of PAPR reduction techniques: Design of DSLM-CT joint reduction technique for advanced waveform," *Soft Comput.*, vol. 24, pp. 11 893–11 907, 2020.

[33] S. Chakravarty and A. Kumar, "PAPR reduction of GFDM signals using encoder-decoder neural network (autoencoder)," *National Academy Sci. Lett.*, vol. 46, no. 3, pp. 213–217, 2023.

[34] A. Kumar, "Analysis of PAPR on NOMA waveforms using hybrid algorithm," *Wireless Personal Commun.*, vol. 132, no. 3, pp. 1849–1861, 2023.
[35] A. Kumar *et al.*, "Reducing PAPR with low complexity filtered NOMA using novel algorithm," *Sustainability*, vol. 14, no. 15, p. 9631, 2022.
[36] S. Ramavath and U. C. Samal, "Theoretical analysis of PAPR companding techniques for FBMC systems," *Wireless Personal Commun.*, vol. 118, no. 4, pp. 2965–2981, 2021.
[37] Z. T. Ibraheem *et al.*, "Boosted PTS method with mu-law companding techniques for PAPR reduction in OFDM systems," *Wireless Personal Commun.*, vol. 124, no. 1, pp. 423–436, 2022.
[38] R. Ghahremani and M. G. Shayesteh, "PAPR and ICI reduction of OFDM signals using new weighting factors from Riemann matrix," *Wireless Personal Commun.*, vol. 84, pp. 1375–1385, 2015.
[39] S. Lipschutz, "On a finite matrix representation of the braid group," *Archiv der Mathematik*, vol. 12, no. 1, pp. 7–12, 1961.
[40] B. Lekouaghet, Y. Himeur, and A. Boukabou, "Improved SLM technique with a new phase factor for PAPR reduction over OFDM signals," in *Proc. IEEE CCSSP*, 2020.
[41] X. Wang, N. Jin, and J. Wei, "A model-driven DL algorithm for PAPR reduction in OFDM system," *IEEE Commun. Lett.*, vol. 25, no. 7, pp. 2270–2274, 2021.
[42] E. Abdullah *et al.*, "Deep learning based asymmetrical autoencoder for PAPR reduction of CP-OFDM systems," *Eng. Sci. Technol. Int. J.*, vol. 50, p. 101608, 2024.
[43] E. E. Eldukhri and M. I. Al-Rayif, "A conditionally applied neural network algorithm for PAPR reduction without the use of a recovery process," *ETRI J.*, 2023.
[44] L. Hao *et al.*, "The extended slm combined autoencoder of the PAPR reduction scheme in DCO-OFDM systems," *Applied Sci.*, vol. 9, no. 5, p. 852, 2019.
[45] L. Li, C. Tellambura, and X. Tang, "Improved tone reservation method based on deep learning for PAPR reduction in OFDM system," in *Proc. IEEE WCSP*, 2019.

Arun Kumar received his Ph.D. in Electronics and Communication Engineering from JECRC University, Jaipur, India. He is an Associate Professor in Electronics and Communication Engineering at New Horizon College of Engineering in Bengaluru, India. Dr. Kumar has a total of 10 years of teaching experience and has published more than 82 research articles in SCI-E and scopus index journals, 2 books and 3 international patents (granted). His research interests are advanced waveforms for 5G mobile communication systems and 5G-based smart hospitals, PAPR reduction techniques in the multicarrier waveform, and spectrum sensing techniques. Dr. Kumar has successfully implemented different reduction techniques for multi-carrier waveforms such as NOMA, FBMC, UFMC, and so on, and has also implemented and compared different waveform techniques for the 5G system. Currently, he is working on the requirements of a 5G-based smart hospital system. He is a Member of the IEEE and a Reviewer for many refereed, indexed journals. He was the Lead Guest Editor of the special issue journal titled "Advanced 5G Communication System for Transforming Healthcare" in the Journal CMC-Computers, Materials and Continua (Q2, SCI, Scopus, Impact Factor: 3.7). He has served as Co-Convenor, Technical Programme Committee (TPC) Member and Reviewer in various international conferences such as ICPCCAI-2019, ICPCCAI-2020, IEEE ISMAC (2018), ESG2018 and so on.

Sumit Chakravarty currently works as an Associate Professor of Electrical Engineering with Kennesaw State University. He also serves as the MSECE Program Coordinator. He completed his doctoral studies from University of Maryland, Baltimore County and his Master of Science from Texas A&M University, Kingsville, both in Electrical Engineering. His PhD dissertation is on analysis of hyperspectral signatures and data. He has multiple peer-reviewed journal publications, conference publications, a book chapter and three granted patents. His area of expertise is wireless communications, AI and signal processing. He has used his expertise in remote sensing by working as a scientist in industry wherein he also worked on other sensor modalities commonly used in remote sensing like multispectral, Lidar, and SAR. This includes working with a cross disciplinary team comprising of specialists from industry, government bodies like NASA, Goddard and academia like University of Maryland. His other industrial experience in engineering and research include working in various roles such as Instrumentation Engineer for Triune Projects, Research Intern at Siemens CAD and Apex Eclipse Communications, Scientist for SGT Inc and Lead Scientist for Honeywell Research (Automatic Control Solutions-Advanced Technology Labs). Some his relevant experience includes instrumentation and plant logic design, noise reduction in communication systems, vibration analysis for equipment health monitoring, flare steam control loop design and modeling, image/video signal segmentation and analysis, and use of statistical techniques for remote sensing and medical CAD applications.

Nishant Gaur working as an Associate Professor of Physics at JECRC University. He has over 23 years of experience in teaching and research. Nishant is currently based in Jaipur, India. He has published several journals and conference papers. His research interest area is 5G, spectrum sensing, optical communication and so on.

Aziz Nanthaamornphong is Associate Professor and serves as the Dean at the College of Computing at Prince of Songkla University's Phuket campus in Thailand. He earned his Ph.D. degree from the University of Alabama, USA. With an extensive academic background, Dr. Nanthaamornphong specializes in empirical software engineering and data science, among other areas. His research significantly contributes to the development of scientific software and leverages data science in the field of tourism. In addition to his core focus, he is also deeply engaged in the study of human-computer interaction, pioneering innovative approaches to foster a beneficial interplay between humans and technology. For correspondence, he can be reached at aziz.n@phuket.psu.ac.th.